Catalysis Science & Technology

Accepted Manuscript

This article can be cited before page numbers have been issued, to do this please use: Z. Hou, W. Ma, Y. Qiao, N. Theyssen, Q. Zhou, D. Li, B. Ding and D. Wang, *Catal. Sci. Technol.*, 2019, DOI: 10.1039/C9CY00056A.

ROYAL SOCIETY OF CHEMISTRY

rsc.li/catalysis

View Article Online
DOI: 10.1039/C9CY00056A

Journal Name

ARTICLE

A mononuclear tantalum catalyst with a peroxocarbonate ligand for olefin epoxidation in compressed CO_2

Received 00th January 20xx,
Accepted 00th January 20xx

DOI: 10.1039/x0xx00000x

www.rsc.org/

Wenbao Ma,[†] Yunxiang Qiao,[‡] Nils Theyssen,[‡] Qingqing Zhou,[†] Difan Li,[†] Bingjie Ding,[†]

Dongqi Wang,*[,§] and Zhenshan Hou*[,†]

A new class of tantalum based-peroxocarbonate ionic liquid ($[P_{4,4,4,4}]_3[Ta(\eta^2\text{-}O_2)_3(CO_4)]$) has been generated through reaction of the pressured CO_2 with $[P_{4,4,4,4}]_3[Ta(O)_3(\eta^2\text{-}O_2)]$ in the presence of H_2O_2 during the reaction process. The newly formed species has been verified by NMR, FT-IR, HRMS and density functional theory (DFT) calculations. The CO_2-induced monomeric peroxocarbonate anion-based ionic liquid is more advantageous than that of the monomeric peroxotantalate analogue for the epoxidation of olefins under very mild condition. Interestingly, the transformation between peroxotantalate and peroxocarbonate species is completely reversible, and CO_2 can actually act as a trigger agent for epoxidation reaction. The further mechanism studies by DFT calculation reveal that the peroxo η^2-O_2 (site *a*) affords higher reactivity towards C=C bond than that of the peroxocarbonate-CO_4 (site *b*). These quantitative illustrations of relationship between structural properties and kinetic consequences enable rational design for an efficient and environmental IL catalyst for the epoxidation of olefins.

Introduction

Transition metal peroxocarbonates have been studied for some time. These transition metals mainly include Rh, Fe, Mn, Pt, etc.[1] They could be prepared through either the reaction between metal peroxo complexes ($[L_nM(\eta^2\text{-}O_2)]$, L=different ligands) and carbon dioxide, or the reaction between carbon dioxide complexes of transition metal and dioxygen.[1c] It has been demonstrated that these compounds are potent candidates for oxygen transfer to oxophiles like phosphines, olefins and ethers.[2] This unique property provides a prospective application in catalytic oxidation. However, these transition metal peroxocarbonates have almost been reported to act as stoichiometric oxidants rather than as highly active catalysts for the oxidation reactions.

Nowadays tantalum has a wide range of applications in the design of catalytic materials.[3] Ta-containing catalysts are increasingly applied in oxidation reactions, most often in the form of solid catalysts based on tantalum oxide or nitride.[4] As for homogeneous systems, the complexes of tantalum have been designed for promoting some important catalytic transformations including hydrogenation of olefins and arenes,[5] hydroaminoalkylation of alkenes[6] and metathesis of alkanes.[7] However, their catalytic performances for the epoxidation of olefins have rarely been explored.[8]

Epoxidation of olefins is a very important organic reaction to produce glycols, glycol ethers, alkanolamines and polymers.[9] The use of H_2O_2 as an oxidant in the epoxidation process is much more promising because water is the only product of H_2O_2 reduction, which is more advantageous than application of environmentally-harmful oxidants, such as peracids and alkylhydroperoxides.[10] The activation of hydrogen peroxide normally requires a metallic catalyst. Microporous titanium silicate zeolite (TS-1) has been widely used to the epoxidation of small olefins with hydrogen peroxide. However, the limited substrate tolerance might be observed.[11] Some supported Ta/Nb oxide catalyst systems also afforded a moderate to good catalytic activity for epoxidation.[12] Additionally, common drawbacks of organometallic complexes, such as their structure instability and the poor recycling performance, largely restrict their application.[13] Thus there still remained a huge challenge of acquiring high catalytic activity and excellent recyclability under mild condition.

Ionic liquids (ILs) are organic salts which have low melting point. ILs have many unusual properties, such as low vapor pressure, wide liquid range, strong polarity, inherent designer nature and recyclability. ILs have realized not only a wide popularity as "green" solvents for synthesis chemistry, but also as powerful catalysts, electrolytes, precursors or additives in some important areas of research as well as in industrial applications.[14] Functionalized ILs are generally named "task-specific ionic liquids" (TSILs), which are prepared through the incorporation of functional groups into the

[†]*Key Laboratory for Advanced Materials, Research Institute of Industrial Catalysis, East China University of Science and Technology, Shanghai 200237, People's Republic of China.*
[‡]*Max-Planck-Institut für Kohlenforschung, Kaiser-Wilhelm-Platz 1, 45470 Mülheim an der Ruhr, Germany.*
[§] *Institute of High Energy Physics, Chinese Academy of Sciences, Beijing 100049, China*
**Z.H.: tel, +86-21-64251686; e-mail, houzhenshan@ecust.edu.cn.*
The Supporting Information is available free of charge on the website. Experimental section, Characterization of the ionic liquid catalysts (HRMS), additional experimental results, and calculated structures, Mulliken atomic charges, bond length and Mayer bond order (PDF).

cation or anion of ILs. The functionalized ILs can impart tailored capabilities to ILs for a specific application, which have attracted a considerable attention.[15]

Recently, we have developed the monomeric peroxotantalate anion-functionalized IL catalysts. The resultant IL catalysts ($[P_{4,4,4,n}]_3[Ta(O)_3(\eta^2\text{-}O_2)]$, $P_{4,4,4,n}$=quaternary phosphonium cation, n=4, 8 and 14) have shown an excellent catalytic activity and selectivity for the epoxidation of allylic alcohols.[16] However, they showed a very poor catalytic activity for the epoxidation of olefins. In this work, we reported that a new tantalum complex containing a peroxocarbonate ligand can be formed *in-situ* by reaction of $[P_{4,4,4,n}]_3[Ta(O)_3(\eta^2\text{-}O_2)]$ with compressed CO_2 in the presence of H_2O_2. The resulting Ta-peroxocarbonate ILs have been characterized in detail by experimental methods including NMR, IR and HRMS as well as DFT calculations. The Ta-peroxocarbonate ILs showed an outstanding activity for the epoxidation of olefins, and CO_2 seemed to act as a trigger reagent here. It was found that the transformation between Ta-peroxocarbonate and peroxotantalate anions was reversible completely, leading to an excellent regeneration of IL catalysts. To the best of our knowledge, this is the first report about Ta-peroxocarbonate complexes and their high catalytic activities towards epoxidation.

Results and Discussion

Herein we reported the preparation of *in-situ* generated tantalum-based peroxocarbonate ILs derived from peroxotantalate based ILs. They were prepared in two steps according to the previously reported method.[16] Firstly, $[P_{4,4,4,n}]OH$ were obtained from $[P_{4,4,4,n}]X$ ($X=Cl^-$ or Br^-) and KOH by ionic exchange, where $[P_{4,4,4,n}]$ represents quaternary phosphonium cations. Then peroxotantalate-based ILs ($[P_{4,4,4,n}]_3[Ta(O)_3(\eta^2\text{-}O_2)]$) were prepared via the reaction of $[P_{4,4,4,n}]OH^-$ with $(NH_4)_3[Ta(O_2)_4]$ in H_2O. After that, tantalum-based peroxocarbonate IL catalysts were obtained *in situ* by reaction of the homoleptic peroxocompound with compressed CO_2.

In order to identify the structure of newly formed species in a compressed carbon dioxide atmosphere, the resulting species has been characterized *in-situ* by high-pressured ^{13}C NMR spectroscopy (Fig. 1). The ^{13}C NMR spectrum of $[P_{4,4,4,4}]_3[Ta(O)_3(\eta^2\text{-}O_2)]$ containing 0.05 mL 30% H_2O_2 (molecular ratio H_2O_2 / IL = 6) in the absence of CO_2 was shown in Fig. 1a. The peaks between 10 and 30 ppm were attributed to quaternary phosphonium cations.[17] In addition, the 0.05 mL 30% H_2O_2 in CD_3OD solution in the presence of 1 MPa CO_2 showed only a signal of dissolved carbon dioxide molecules at about 125.9 ppm (Fig. 1b). Nevertheless, the introduction of $[P_{4,4,4,4}]_3[Ta(O)_3(\eta^2\text{-}O_2)]$ into CD_3OD solution containing 0.05 mL 30% H_2O_2 in the presence of 1.0 MPa CO_2 led to the appearance of two new peaks at 160.9 and 169.8 ppm. The former one is attributed to HCO_3^-,[18] while the latter one is assigned to the peroxocarbonate species (Fig. 1c).[1i] Moreover, when the pressure of carbon dioxide was increased to 2 MPa, the peak of dissolved carbon dioxide could again be observed at 125.9 ppm (Fig. 1d). It was noting that the peak at about 158.4 ppm ascribed to HCO_4^- species was not observed under the present conditions, likely due to low H_2O_2 concentration.[19]

These results indicated clearly that the peroxotantalate-based IL $[P_{4,4,4,4}]_3[Ta(\eta^2\text{-}O_2)_4]$ indeed could react with CO_2 to form a new Ta-peroxocarbonate species.

Next, FT-IR spectra of the new formed IL were presented according to following procedures. 0.5 mmol of $[P_{4,4,4,4}]_3[Ta(O)_3(\eta^2\text{-}O_2)]$ was mixed with 1 mL methanol and 5 mmol aqueous hydrogen peroxide. After stirring for 10 min at 0 °C, diethyl ether was poured into the solution rapidly to precipitate the oxidizing species ($[P_{4,4,4,4}]_3[Ta(\eta^2\text{-}O_2)_4]$).[16] This was then carefully washed with 5 mL cold diethyl ether in a sequential manner. After that, the oxidizing species was characterized by *in-situ* FT-IR spectra in an atmosphere of compressed CO_2 for the sake of comparison. The spectra are shown in Fig. 2. The band at about 1655 cm^{-1} in $KHCO_3$ was characteristic for the ν(C=O) of HCO_3^- (Fig. 2a).[20] No obvious adsorption band around 1500 and 2000 cm^{-1} was observed for gas CO_2 (Fig. 2b), which was coincident with that reported in the literature.[21] Moreover, the homoleptic complex ($[P_{4,4,4,4}]_3[Ta(\eta^2\text{-}O_2)_4]$) showed a band at 1644 cm^{-1}, which could be attributed to the adsorption of water molecules on the IL catalyst (Fig. 2c).[22] When the oxidizing species ($[P_{4,4,4,4}]_3[Ta(\eta^2\text{-}O_2)_4]$) was treated with 2.0 MPa CO_2 for 1 min *in-situ*, two new bands at 1683 cm^{-1} and 1282 cm^{-1} appeared and increased with time. These could be attributed to the ν(C=O) and ν(C-O), respectively which resulted from the vibration of peroxocarbonate species (Fig. 2c-2f).[1f,1i]

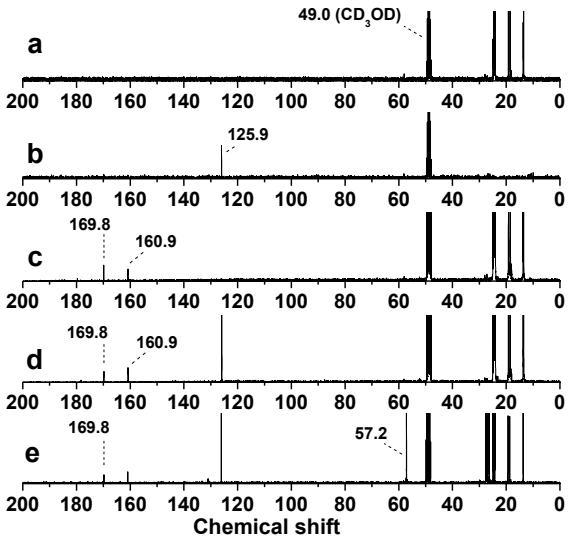

Fig. 1 ^{13}C NMR spectra of peroxotantalate-based ILs in CD_3OD (49.0 ppm): (a) $[P_{4,4,4,4}]_3[Ta(O)_3(\eta^2\text{-}O_2)]$ containing 0.05 mL 30% H_2O_2 in the absence of CO_2. (b) Sole CD_3OD containing 0.05 mL 30% H_2O_2 in the presence of 1.0 MPa CO_2. (c) $[P_{4,4,4,4}]_3[Ta(O)_3(\eta^2\text{-}O_2)]$ containing 0.05 mL 30% H_2O_2 in the presence of 1.0 MPa CO_2. (d) $[P_{4,4,4,4}]_3[Ta(O)_3(\eta^2\text{-}O_2)]$ containing 0.05 mL 30% H_2O_2 in the presence of 2.0 MPa CO_2. (e) Cyclooctene was added to the CD_3OD solution (d) untill the epoxidation reaction was completed. The signal at 169.8 ppm arisen from Ta-peroxocarbonate species was still observed clearly and peak at 57.2 ppm was contributed to the resonance signal of cyclooctene oxide.

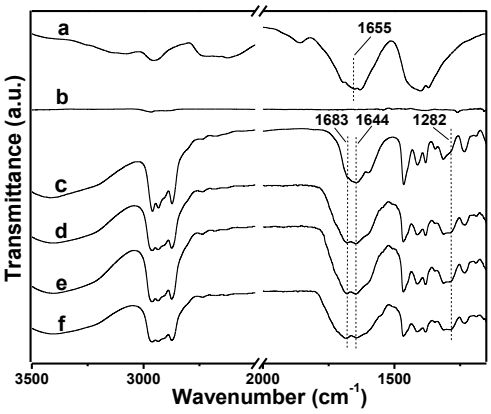

Fig. 2 In situ high-pressured FT-IR spectra of (a) $KHCO_3$ in the absence of CO_2. (b) 2.0 MPa CO_2 in the absence of catalyst. (c) $[P_{4,4,4,4}]_3[Ta(\eta^2\text{-}O_2)_4]$ in the absence of CO_2. (d) $[P_{4,4,4,4}]_3[Ta(\eta^2\text{-}O_2)_4]$ under 2.0 MPa CO_2 after 1 min. (e) $[P_{4,4,4,4}]_3[Ta(\eta^2\text{-}O_2)_4]$ under 2.0 MPa CO_2 after 3 min. (f) $[P_{4,4,4,4}]_3[Ta(\eta^2\text{-}O_2)_4]$ under 2.0 MPa CO_2 after 5 min.

Then the IL catalyst ($[P_{4,4,4,4}]_3[Ta(O)_3(\eta^2\text{-}O_2)]$) was stirred for 20 min in methanol containing hydrogen peroxide under an CO_2 atmosphere of 2.0 MPa at 0 °C. After that, the solution was analyzed by HRMS (Fig. S1). The ESI-MS of $[P_{4,4,4,4}]_3[Ta(\eta^2\text{-}O_2)_4]$ in CH_3OH dealt with 2 MPa CO_2 afforded an ion centered at 306.9283 m/z corresponding to $[TaO_3(CO_4)H_2]^-$ species, which was probably due to the decomposition of the labile peroxo bonds of intermediate during HRMS experiments.

Based on the above result, we can conclude that the active intermediate $[P_{4,4,4,4}]_3[Ta(\eta^2\text{-}O_2)_4]$ could react with carbon dioxide to afford a new species. In order to identify further how much CO_2 can be incorporated into the Ta-peroxocarbonate IL, $[P_{4,4,4,4}]_3[Ta(\eta^2\text{-}O_2)_4]$ (2.752 g, 2.5 mmol) was purged continuously with 3 MPa CO_2 at 0 °C. The amount of CO_2 absorbed into the IL was determined at regular intervals by the electronic balance with an accuracy of ±0.1 mg. The results are shown in Fig. 3 (run 1). It was found that the weight of ionic liquid increased gradually with time until the absorption capacity of CO_2 reached up to 2.3 mmol. After that, the resulting Ta-peroxocarbonate IL was dealt under reduced pressure condition at 50 °C for 2 h, and then was reactivated with H_2O_2. The $[P_{4,4,4,4}]_3[Ta(\eta^2\text{-}O_2)_4]$ was purged continuously with 3 MPa CO_2 again and the results are shown in Fig. 3 (run 2). Similar steps were repeated another two times. It can be seen that the molar ratio of the absorbed CO_2 to $[P_{4,4,4,4}]_3[Ta(\eta^2\text{-}O_2)_4]$ was equivalent to *ca*. 1, indicating that the *in-situ* prepared Ta-peroxocarbonate anionic species only contained one peroxocarbonate ligand, which was also in good agreement with that of HRMS. The amount of CO_2 absorption by IL did not decreased obviously in the whole recycles (Fig. 3), indicating that the structural transformation between Ta-peroxocarbonate and peroxotantalate anions is completely reversible.

The potential formation of Ta-peroxocarbonate and peroxotantalate anions and their relative thermodynamic stabilities were further evaluated by DFT calculations. Starting from $TaO_3(\eta^2\text{-}O_2)^{3-}$, these species were considered to be produced via the channels tabulated in Table 1. The geometries of these species are collected in Fig. S2. The oxidation of $TaO_3(\eta^2\text{-}O_2)^{3-}$ by H_2O_2 to produce $Ta(\eta^2\text{-}O_2)_4^{3-}$ was calculated to be a strongly exothermic process. In the CO_2 atmosphere, the tantalum tetraperoxide may accommodate a molecule of CO_2 to afford the Ta-peroxocarbonate anion ($Ta(\eta^2\text{-}O_2)_3(CO_4)^{3-}$) with a loss of free energy of 21.04 kJ/mol (Table 1), which may further react with H_2O_2 to give $TaO(\eta^2\text{-}O_2)_2(CO_4)^{3-}$, $TaO_2(\eta^2\text{-}O_2)(CO_4)^{3-}$ and $TaO_3(CO_4)^{3-}$ in a stepwise manner. According to calculations, it is also possible for a second molecule of CO_2 to insert into the Ta-peroxocarbonate anion, but with much less exothermicity than the above-mentioned channels. This agrees with the experimental measurements that the Ta-biperoxocarbonate species were not detected. As a result, according to the above experimental and theoretical results, the new tantalum-containing species produced from the oxidation of $[P_{4,4,4,4}]_3[Ta(O)_3(\eta^2\text{-}O_2)]$ by H_2O_2 in our experiment under high pressure CO_2 atmosphere is proposed as $[P_{4,4,4,4}]_3[Ta(\eta^2\text{-}O_2)_3(CO_4)]$ (Scheme 1).

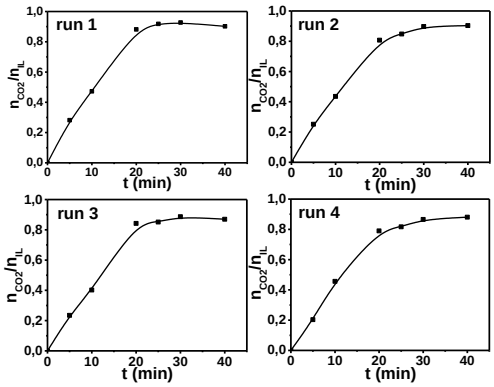

Fig. 3 CO_2 absorption recycles of $[P_{4,4,4,4}]_3[Ta(\eta^2\text{-}O_2)_4]$. In each run, CO_2 was absorbed at 0 °C and 3.0 MPa, and desorbed at 50 °C under the vacuum.

Catalytic Performance

As reported previously, the peroxocarbonate complexes are potential oxidants in general, which could cause oxygen transfer from the peroxocarbonate moiety to the oxophiles. Therefore, the catalytic activity of the new Ta-peroxocarbonate species has been examined under a variety of reaction conditions. The addition of CO_2 has a tremendous effect on the reaction. As shown in Fig. 4a, no cyclooctene conversion was observed in the absence of CO_2 with $[P_{4,4,4,4}]_3[Ta(O)_3(\eta^2\text{-}O_2)]$ catalyst. However, the conversion of cyclooctene increased sharply with pressure and achieved a maximum value of 87.2% around 2.0 MPa CO_2, which was about twice as much than that the yield at atmospheric pressure (40.2%). A further pressure increase over 2.0 MPa caused a lower conversion of cyclooctene. It's noting that there was no phase separation when the pressure was below 4.0 MPa. Therefore a lower conversion could be explained by a substrate dilution effect in the CO_2-swollen liquid reaction phase.[23] Furthermore, the effect of temperature on

Table 1 The Reaction (free) energies (in kJ/mol) in the formation of possible Ta-peroxocarbonate and peroxotantalate anionic species via oxidation or CO_2 insertion reaction

Reactions	ΔE_{bond}	ΔG
$TaO_3(\eta^2\text{-}O_2)^{3-} + 3H_2O_2 \rightarrow Ta(\eta^2\text{-}O_2)_4^{3-} + 3H_2O$	-237.58	-233.19
$Ta(\eta^2\text{-}O_2)_4^{3-} + CO_2 \rightarrow Ta(\eta^2\text{-}O_2)_3(CO_4)^{3-}$	-77.07	-21.04
$Ta(\eta^2\text{-}O_2)_3(CO_4)^{3-} \rightarrow TaO(\eta^2\text{-}O_2)_2(CO_4)^{3-} + 1/2O_2$	-14.30	-51.06
$Ta(\eta^2\text{-}O_2)_3(CO_4)^{3-} + H_2O_2 \rightarrow TaO(\eta^2\text{-}O_2)_2(CO_4)^{3-} + H_2O + O_2$	-107.98	-167.03
$Ta(\eta^2\text{-}O_2)_3(CO_4)^{3-} + 2H_2O_2 \rightarrow TaO_2(\eta^2\text{-}O_2)(CO_4)^{3-} + 2H_2O + 2O_2$	-221.23	-330.25
$Ta(\eta^2\text{-}O_2)_3(CO_4)^{3-} + 3H_2O_2 \rightarrow TaO_3(CO_4)^{3-} + 3H_2O + 3O_2$	-345.73	-493.43
$Ta(\eta^2\text{-}O_2)_3(CO_4)^{3-} + CO_2 \rightarrow Ta(\eta^2\text{-}O_2)_2(CO_4)_2^{3-}\text{-I}$	-72.64	-20.66
$Ta(\eta^2\text{-}O_2)_3(CO_4)^{3-} + CO_2 \rightarrow Ta(\eta^2\text{-}O_2)_2(CO_4)_2^{3-}\text{-II}$	-71.14	-18.78
$TaO_2(\eta^2\text{-}O_2)(CO_4)^{3-} + CO_2 \rightarrow TaO_2(CO_4)_2^{3-}\text{-I}$	-46.04	7.61
$TaO_2(\eta^2\text{-}O_2)(CO_4)^{3-} + CO_2 \rightarrow TaO_2(CO_4)_2^{3-}\text{-II}$	-71.14	-18.78

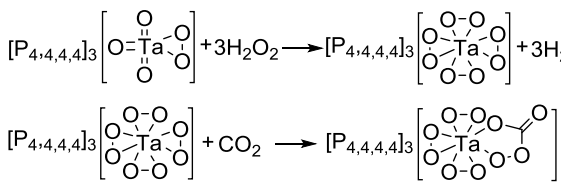

Scheme 1 The structure evolution of $[P_{4,4,4,4}]_3[Ta(O)_3(\eta^2\text{-}O_2)]$ in the presence of hydrogen peroxide under compressed CO_2.

the reaction has also been investigated and the result was shown in Fig. 4b. It can be seen that a maximum conversion of cyclooctene was achieved at 40 °C. At a higher temperature, the conversion of cyclooctene decreased, probably due to decomposition of H_2O_2 and/or active Ta-peroxocarbonate species. This reveals that both the presence of CO_2 and appropriate reaction temperature are very crucial for the improvement of activity.

The epoxidation of cyclooctene was performed in different reaction media in order to examine the influence of different solvents. A poor conversion has been obtained in dichloromethane and ethyl acetate (Table S1, entries 1 and 2), which was probably due to the biphasic state during the course of reaction. The reaction also displayed a low activity in acetonitrile (Table S1, entry 3). However, the conversion of cyclooctene increased significantly up to 42.3% and 87.2%, in ethanol and methanol, respectively (Table S1, entries 3-5), showing that the present epoxidation reaction is favored in strong polar protic solvents. Previous reports from our group and from other authors have demonstrated that the hydrogen bonding interaction between polar protic solvents and the peroxometalate specie activates the peroxo bond, resulting in a lower barrier for epoxidation.[24] Futhermore, tert-butyl hydroperoxide (TBHP) has also been tested as an oxidant. The results showed that the epoxidation of olefins did not proceed with

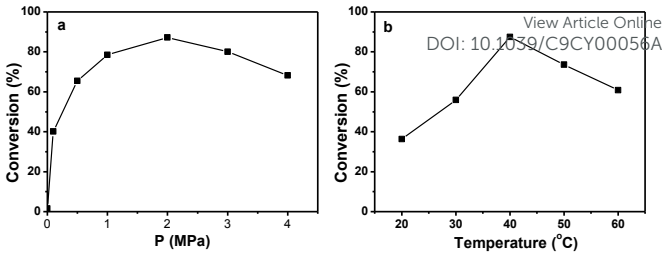

Fig. 4 (a) Effect of CO_2 pressure on epoxidation of cyclooctene. Reaction condition: 2.0 mmol cyclooctene, 2.0 mmol H_2O_2, 0.05 mmol $[P_{4,4,4,4}]_3[Ta(O)_3(\eta\text{-}O_2)]$, 2.5 mL CH_3OH, 40 °C. (b) Effect of temperature on epoxidation of cyclooctene. Reaction condition: 2.0 mmol cyclooctene, 2.0 mmol H_2O_2, 0.05 mmol $[P_{4,4,4,4}]_3[Ta(O)_3(\eta\text{-}O_2)]$, 2.0 MPa CO_2, 2.5 ml CH_3OH.

TBHP under the similar reaction conditions or slightly higher reaction temperatures (Table S2, entries 1-3). This indicated that the present Ta-peroxocarbonate species cannot activate tert-butyl hydroperoxide in the desired manner under the present conditions.

Moreover, the epoxidation of cyclooctene was investigated further by variation of the catalyst structure (Table 2). In the absence of catalysts (entry 1), almost no conversion of cyclooctene was observed. The same holds for $[P_{4,4,4,4}]Br$ (entry 2) and $KHCO_3$ (entry 3), indicating that the catalytic activity originates from the tantalum-containing anionic part. It was worth noting that the epoxidation did not proceed at all without CO_2 or under 2.0 MPa N_2 atmosphere in the presence of $[P_{4,4,4,4}]_3[Ta(O)_3(\eta^2\text{-}O_2)]$ (entries 4 and 5). In contrast, the introduction of 2.0 MPa CO_2 to $[P_{4,4,4,4}]_3[Ta(O)_3(\eta^2\text{-}O_2)]$ solution resulted in a fantastic increase of conversion up to 87.2% (entry 6). $(NH_4)_3[Ta(O_2)_4]$ showed a poor solubility in methanol, resulting in a liquid-solid biphasic system, which could account for a poor cyclooctene conversion (entry 7). A

Table 2 Epoxidation of cyclooctene with different catalysts in the presence of the pressured CO_2[a]

entry	catalysts	Con. /%[b]	Sel./% epoxide	Sel./% others[c]
1	None	1.1	≥ 99	< 1
2	$[P_{4,4,4,4}]Br$	2.3	≥ 99	< 1
3	$KHCO_3$	3.4	≥ 99	< 1
4	$[P_{4,4,4,4}]_3[Ta(O)_3(\eta^2\text{-}O_2)]$[d]	2.3	≥ 99	< 1
5	$[P_{4,4,4,4}]_3[Ta(O)_3(\eta^2\text{-}O_2)]$[e]	2.0	≥ 99	< 1
6	$[P_{4,4,4,4}]_3[Ta(O)_3(\eta^2\text{-}O_2)]$	87.2	≥ 99	< 1
7	$(NH_4)_3[Ta(O_2)_4]$	4.5	≥ 99	< 1
8	$[P_{4,4,4,8}]_3[Ta(O)_3(\eta^2\text{-}O_2)]$	78.0	≥ 99	< 1
9	$[P_{4,4,4,14}]_3[Ta(O)_3(\eta^2\text{-}O_2)]$	64.9	≥ 99	< 1

[a]Reaction conditions: substrate (2 mmol), H_2O_2 (2.0 mmol, 30% aqueous solution), catalyst (0.05 mmol), 40 °C, 12 h, 2.5 mL CH_3OH, 2.0 MPa CO_2. [b]GC conversion with dodecane as an internal standard. Conversion=$([R_0]-[R])/[R_0]$, $[R_0]$ refer to the initial concentration of cyclooctene, [R] refer to the concentration after the reaction. [c]Refer to cyclooctanediol. [d]without CO_2. [e]2 MPa N_2 instead of 2 MPa CO_2.

View Article Online
DOI: 10.1039/C9CY00056A

moderate to good activity could be achieved using $[P_{4,4,4,8}]_3[Ta(O)_3(\eta^2\text{-}O_2)]$ and $[P_{4,4,4,14}]_3[Ta(O)_3(\eta^2\text{-}O_2)]$ catalysts under the pressured CO_2 (entries 8 and 9), which showed that the decent structure of the phosphonium cation has an additional influence on the catalytic activity. The addition of CO_2 may affect the acidity of the reaction mixture. It has been reported that acidity could exert an impact on the catalytic performance of transition metal peroxo complexes.[25] Nevertheless, the control experiments indicated that almost no conversion of cyclooctene was observed even if 0 to 0.03 mmol HNO_3 was added to reaction system. This revealed that the acidity wasn't a decisive factor in the present epoxidation reaction.

Sequentially, the reaction kinetics was investigated in order to gain an insight into the pathways of hydrogen peroxide activation and olefin epoxidation. The effects of stirring speed and catalyst amount on the reaction rate have been screened to exclude the presence of diffusion limitations prior to kinetic studies. The results are shown in Fig. S3. A stirring of no less than 800 rpm was needed. If the molar ratio of substrate and IL catalyst ($n_{sub.}/n_{cat.}$) was less than 40, the conversion of cyclooctene remained almost constant.

With regard to the results of other groups and our previous research, the rate of epoxidation of olefins showed a linear dependence on the concentration of substrate and independence on the concentration of hydrogen peroxide at low concentrations.[16,26] Next, the reaction kinetics of the catalyst were investigated and the activation energy was attained. The results are shown in Fig. 5, where the reaction rate constant was determined from the experimental data by assuming pseudo-first-order reaction kinetics. The activation energy (Ea) of the catalyst under the present condition is about 43.4 $kJ\cdot mol^{-1}$, which is indeed lower than previously reported values for metal-based catalysts where activation energies are in the range of 49-100 $kJ\cdot mol^{-1}$.[27]

In the next step, a series of olefins were tested in order to examine the substrate scope of the present IL catalyst. The results were summarized in Table 3. Conversions between 87.2% and 96.8% were obtained in the epoxidation of cyclic olefins (Table 3, entries 1-4). An even higher conversion of about 98.6% could be

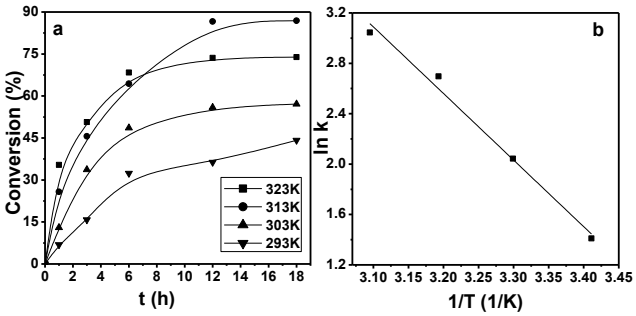

Fig. 5 (a) Conversion/time profiles of epoxidation reactions catalyzed by $[P_{4,4,4,4}]_3[Ta(O)_3(\eta^2\text{-}O_2)]$ at different temperatures. (b) Arrhenius plots for the epoxidation reaction of cyclooctene and H_2O_2. The observed rate constants (k) were calculated with the initial rates by Fig. 5a at different temperatures. Reaction conditions: cyclooctene (2.0 mmol), H_2O_2 (2.0 mmol), $[P_{4,4,4,4}]_3[Ta(O)_3(\eta^2\text{-}O_2)]$ (0.05 mmol), 2.0 MPa CO_2, 2.5 mL CH_3OH.

Table 3 Epoxidation of different substrates with $[P_{4,4,4,4}]_3[Ta(O)_3(\eta^2\text{-}O_2)]$ under a CO_2 atmosphere of 2.0 MPa[a]

entries	substrates	t /°C	T /h	Con. /%[b]	Sel./% epoxide	Sel./% others
1		40	12	87.2	≥99	<1
2[c]		40	12	98.6	≥99	<1
3		40	12	88.7	95.0	5.0
4		40	12	96.8	≥99	<1
5[d]	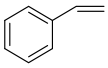	40	12	67.5	67.0	33.0
6[d]	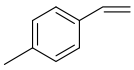	40	12	65.4	64.2	35.8
7[d]	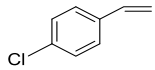	40	12	50.2	59.6	40.4
8	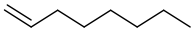	40	12	9.7	≥99	<1
9	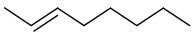	40	12	28.1	≥99	<1
10[e]		0	1.5	98.9	≥99	<1
11[e]	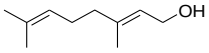	0	3.5	96.7	≥99	<1
12[e]	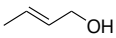	0	3.5	94.2	≥99	<1
13[e]	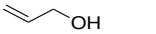	0	5.5	72.5	≥99	<1

[a]Reaction conditions: substrates (2.0 mmol), H_2O_2 (2.0 mmol, 30% aqueous solution), catalyst (0.05 mmol), 40 °C, 2.5 mL of CH_3OH, 2 MPa CO_2. [b]GC conversion with dodecane as an internal standard. [c]H_2O_2 (2.4 mmol, 30% aqueous solution). [d]The corresponding aromatic aldehydes (benzaldehyde, *p*-tolualdehyde, and *p*-chlorobenzaldehyde) have been detected as the main by-products. [e]Solvent-free condition.

reached if slightly more H_2O_2 was used (entry 1 *vs* 2). In addition, the catalyst also transformed vinyl arenes into epoxides, although a small amount of benzylic aldehydes (benzaldehyde, p-olualdehyde, and p-chlorobenzaldehyde) were detected as the main by-products (entries 5-7). The catalyst also afforded an excellent selectivity for epoxidation of linear terminal alkenes in spite of a low reactivity (entry 8). A slightly higher reactivity can be observed for linear internal alkenes (entry 9), which is consistent with the mechanism involving facile transfer of electrophilic oxygen from the active peroxo species of the IL catalyst to electron-rich olefins to afford epoxides. Notably, the IL catalyst system also displayed an excellent catalytic activity and selectivity for the epoxidation of allylic alcohols even at 0 °C (entries 10-13). The amount of residual H_2O_2 was also measured. For example, a residue of 2%-5% (entries 1-4 and 10-13), 17%-21% (entries 5-7) and 38%-45% (entries 8 and 9) initial H_2O_2 can be found after reaction, respectively. These observations indicated that those electron-rich olefins indeed owned high H_2O_2 utilization efficiency. Compared to the reported Mn/bicarbonate catalyst

system,[13g] the present system afforded a higher TOF and oxidant utilization efficiency.

The recyclability of $[P_{4,4,4,4}]_3[Ta(O)_3(\eta^2\text{-}O_2)]$ has been examined alternately in pressured CO_2 or N_2 and the results are shown in Fig. 6. It was found that the IL catalyst maintained high catalytic activity for at least five cycles in the compressed CO_2. However, once CO_2 was replaced by N_2 in an alternating manner, the conversion decreased by at least one order of magnitude each time under otherwise identical reaction conditions. This interesting observation revealed that CO_2 could indeed act as a trigger reagent for such epoxidations. The conversion between $[P_{4,4,4,4}]_3[Ta(\eta^2\text{-}O_2)_4]$ and $[P_{4,4,4,4}]_3[Ta(\eta^2\text{-}O_2)_3(CO_4)]$ is fully reversible as shown previously in Fig. 3, and the $[Ta(\eta^2\text{-}O_2)_3(CO_4)]^{3-}$ anion is believed to be the catalytically active species here.

Reaction Mechanism

On the basis of the above research, it can be concluded that the parent IL anion $[Ta(O)_3(\eta^2\text{-}O_2)]^-$ is easily converted into $[Ta(\eta\text{-}O_2)_3(CO_4)]^{3-}$ in the presence of H_2O_2 and compressed CO_2. In principle, there are two types of sites that potentially insert one O atom into the C=C bond to give the epoxide product: the peroxo η-O_2 (site *a*) and the peroxocarbonate-CO_4 (sites *b*), i.e. the epoxidation may proceed along the two pathways as shown in (1) and (2):

$$\text{(site } a\text{) } Ta(\eta^2\text{-}O_2)_3(CO_4)^{3-} + C_8H_{14} \rightarrow TaO(\eta^2\text{-}O_2)_2(CO_4)^{3-} + C_8H_{14}O \quad \textbf{(1)}$$

$$\text{(site } b\text{) } Ta(\eta^2\text{-}O_2)_3(CO_4)^{3-} + C_8H_{14} \rightarrow Ta(\eta^2\text{-}O_2)_3(CO_3)^{3-} + C_8H_{14}O \quad \textbf{(2)}$$

In order to elucidate this, density functional theory was used to locate the stationary points along the pathways for the two sites. As can be seen in Fig. S4 for both pathways, the C=C bond of the cyclooctene substrate does not interact with the active sites directly. When approaching the transition states (TSa and TSb), the length of the peroxo bond that deliver one of its O atom to the cyclooctene increases by 0.336 (TSa) and 0.305 (TSb) Å. The migrating O atom (O6 in TSa, and O1 in TSb) attaches to the C=C bond more symmetrically in TSa than in TSb, suggesting a higher propensity for the reaction at site *a* to happen synchronously than that at site *b*.

Energetically, the activation energy of pathway *a* was calculated to be 75.4 kJ mol^{-1}, which is 39.1 kJ mol^{-1} lower than that to the pathway *b* (Table 4). We note that these values are larger than the experimentally measure value (43.4 kJ/mol). This deviation is understandable for two reasons: One might be an insufficient description of the solvent effect and the other is believed to appear on the sole calculation of this single elementary reaction step only.

Mulliken population analysis was carried out to further understand the energetic difference between the two pathways. As can be seen in Table 4, in the reactant state, the HOMO for site *a* is constituted by the π* orbitals of peroxide ligands that coordinated with Ta in a *η*-manner. The LUMO is determined to be the σ* orbital of the peroxo group of the carbonate peroxide ligand. When the substrate accesses site *b*, the π orbital of the C=C bond interacts with the LUMO orbital of $Ta(\eta^2\text{-}O_2)_3(CO_4)^{3-}$. The reorganization of the frontier orbitals cleaves the $\sigma_{O\text{-}O}$ and $\pi_{C=C}$ bonds to facilitate the formation of C-O bonds and afford the epoxide product. In the reaction at the site *a*, the π orbital of the C=C bond interacts with the σ* orbital of η^2-O_2 ligand to demolish the O-O bond (Table 4).

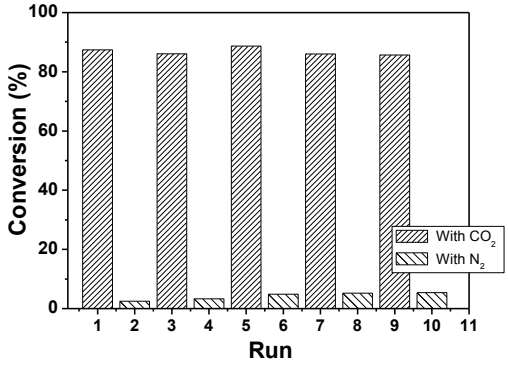

Fig. 6 Recyclability of the $[P_{4,4,4,4}]_3[Ta(O)_3(\eta^2\text{-}O_2)]$ catalyst in the presence of the pressured CO_2 or N_2. Reaction conditions: substrate (2 mmol), H_2O_2 (2 mmol, 30% aqueous solution), $[P_{4,4,4,4}]_3[Ta(O)_3(\eta^2\text{-}O_2)]$ (0.05 mmol), 2.5 mL CH_3OH, 12 h, 40 °C, 2.0 MPa CO_2 at run 1, 3, 5, 7 and 9; 2.0 MPa N_2 at run 2, 4, 6, 8 and 10.

Table 4 Frontier orbitals (isovalue 0.05a.u.) and relative (free) energies (in kJ mol^{-1}) for the epoxidation at sites *a* and *b*. Data in parentheses are Gibbs Free Energy changes[a]

	Site *a*		Site *b*	
	HOMO	LUMO	HOMO	LUMO
RC[b]	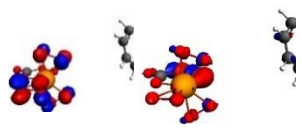		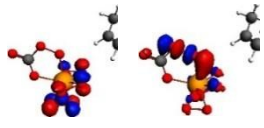	
TS[b]	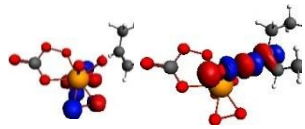		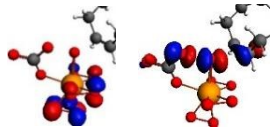	
PC[b]	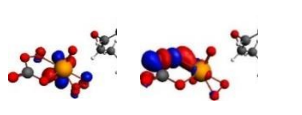		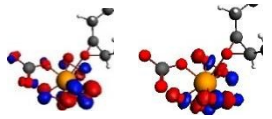	
$\Delta G^{\neq}$ ($\Delta E^{\neq}$)	75.4 (86.6)		114.5 (108.0)	
ΔG (ΔE)	-148.3 (-135.9)		-130.3 (-140.9)	

[a]$\Delta E^{\neq} = E_{TS} - E_{RC}$; $\Delta E = E_{PC} - E_{RC}$; $\Delta G^{\neq} = G_{TS} - G_{RC}$, $\Delta G = G_{PC} - G_{RC}$. [b]The atoms of the cyclooctene substrate in RC, TS and the corresponding epoxide product in PC which are far away from the reaction center and have no contribution to the HOMO and LUMO orbitals and therefore not shown for simplicity.

Table 5 Bond energy decomposition (kJ/mol) of TSa and TSb

View Article Online
DOI: 10.1039/C9CY00056A

	Steric interaction			Orbital interaction				Solvation	
	Pauli	Elec.	Sum	Kinetic	Coulomb	XC	Sum	screening	c+d[a]
TSa	6.26E+4	-1.46E+4	4.80E+4	-1.90E+5	1.17E+5	5.34E+3	-6.71E+4	-1.76E+3	8.24E+0
TSb	6.25E+4	-1.46E+4	4.79E+04	-1.88E+5	1.16E+5	5.25E+3	-6.71E+4	-1.71E+3	8.15E+0
Δ(a-b)	124.67	-41.57	83.10	-1034.29	878.60	92.09	-63.61	-49.51	0.08

[a] The sum of contributions of cavitation and dispersion.

Bond energy decomposition of the two transition states according to Morokuma[28] and Ziegler[29], as shown in Table 5, indicates that the reaction at site *a* benefits more from orbital interaction and solvation while feels more impedance from the steric interaction, mainly by the Pauli repulsion. This is consistent with the orbital analysis, as seen in Table 4, where there is more overlap between the σ* orbital of the peroxo moiety and the π orbital of cyclooctene in the TS along the reaction at site *a* than at site *b*. The composite effect of these interactions moderately favor the epoxidation of cyclooctene to happen at the site *a*.

We have also analyzed the atomic charges of key atoms and bond properties of key bonds in $[Ta(\eta^2\text{-}O_2)_3(CO_4)]^{3-}$. As shown in Fig. S5 and S6, upon the insertion of CO_2 into the Ta-O bond, the atomic charge of O^{peroxo} becomes more positive, and the covalency of Ta-O^{peroxo} bond is enhanced. These features leads to a higher reactivity of Ta-O^{peroxo} bond in $[Ta(\eta^2\text{-}O_2)_3(CO_4)]^{3-}$ than in $[Ta(\eta^2\text{-}O_2)_4]^{3-}$. We also note that in $[Ta(\eta^2\text{-}O_2)_3(CO_4)]^{3-}$, the O^{peroxo} atoms (site *a*) of the η^2-peroxide ligand carry similar atomic charge as the $O^{carboperox}$ atom (site *b*), suggesting the two sites have close eletrophilicity, which may thus not be the determining factor responsible for their distinct reactivity.

The analysis of the key bonds indicates that the O-O distance in the η^2-peroxide ligand (1.51 Å) is marginal longer than that in the peroxocarbonate group (1.48 Å) (Fig. S6). This shows that it is easier to break the former bond than the latter one. As both O atoms are involved in a peroxo bond and appear in the first coordination shell of Ta, it is conceivable that the direct contact with Ta may influence their reactivity towards the epoxidation of olefin significantly. The examination of the bond nature indicates that Ta-O^{perox} has a bigger MBO (Mayer bond order) of 0.70 than Ta-$O^{carboperox}$ (0.55) (Fig. S6), indicating more significant covalency of the former than the latter, and stronger ionic feature of the latter. In organometallic chemistry, a highly reactive M-E (M: metal atom, E: non-metallic atom) is often displaying a relative weak polarity. This suggests that the Ta-O^{perox} site may have stronger reactivity than the Ta-$O^{carboperox}$ site, which is consistent with the calculated energy barriers of the epoxidation at the two sites. In another paralleling experiment, as shown in Fig. 1e, it can be seen that the peak at 169.8 ppm attributed to Ta-peroxocarbonate species was still observed clearly in the CD_3OD solution after the reaction was completed. This demonstrated that the reaction proceeded mostly at the peroxo η^2-O_2 (site a) instead of the peroxocarbonate-CO_4 (sites b).

Based on the catalyst characterization, the activity test of the epoxidation reaction and DFT calculations, a reaction mechanism is proposed accordingly. The anion $[Ta(O)_3(\eta^2\text{-}O_2)]^{3-}$ is oxidized to the tetraperoxotantalate species $[Ta(\eta^2\text{-}O_2)_4]^{3-}$ in the excess of hydrogen peroxide, which could accommodate one molecule of CO_2 to generate the tantalum-based peroxocarbonate species $[Ta(\eta^2\text{-}O_2)_3(CO_4)]^{3-}$ under compressed CO_2. The Ta-peroxocarbonate complexes were identified as the active species for olefin epoxidation. There are two types of sites (e.g., η^2-O_2^{2-} and the CO_4^{2}) in the tantalum-based peroxocarbonate anion ($[Ta(\eta\text{-}O_2)_3(CO_4)]^{3-}$) that are potentially able to insert one O atom into the C=C bond to give the epoxide product. However, according to the DFT calculations and experiments, the peroxo site η^2-O_2 afforded a higher reactivity towards the epoxidation of the C=C bond. As a result, the epoxide is produced via a three-membered ring transition state. $[TaO(\eta^2\text{-}O_2)_2(CO_4)]^{3-}$ is formed and then is reconverted to replenish the oxidizing species with hydrogen peroxide and complets the catalytic cycle (Scheme 2). As we have indicated in the previous work, the quaternary phosphonium cations could not only play a crucial role in balancing the negatively charged Ta-peroxocarbonate anion, but also ensure a homogeneous phase in the course of the reaction.

Our previous research illustrated that the coordination between the α-hydroxy acid and the peroxoniobate anion causes the O^{peroxo} atom in $[Nb(OO)_2LA]^-$ (LA=lactic acid) to bear a less negative charge than that of $[Nb(O\text{-}O)_2(OOH)_2]^-$.[24b] The lower electron density of the reactive center (O atom) exhibits a higher reactivity towards to C=C bond owing to the electrophilic addition mechanism of the epoxidation process. Actually, we considered that CO_2 played a quite similar role to that of α-hydroxy carboxylic acid, the insertion of CO_2 makes the atomic charge of O^{peroxo} atoms in $[Ta(\eta^2\text{-}O_2)_3(CO_4)]^{3-}$ more positive, which hence gives a higher reactivity than $[Ta(\eta^2\text{-}O_2)_4]^{3-}$. However, CO_2 can *in-situ* generate or remove peroxocarbonate ligand reversibly. The use of CO_2 is more flexible and eco-friendly, as compared with that of organic acids.

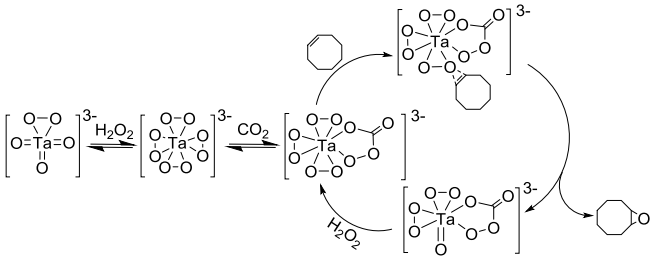

Scheme 2 Proposed mechanism for epoxidation of cyclooctene with H_2O_2 catalyzed by peroxotantalate-based ionic liquids in compressed CO_2.

Conclusion

In summary, we have demonstrated that the tantalum-based peroxocarbonate species $[P_{4,4,4,4}]_3[Ta(\eta^2\text{-}O_2)_3(CO_4)]$ can be *in-situ* generated from the reaction of $[P_{4,4,4,4}]_3[Ta(O)_3(\eta^2\text{-}O_2)]$ with the compressed CO_2 in the presence of H_2O_2. The structure of peroxocarbonate species have been verified experimentally by NMR, FT-IR, HRMS and DFT calculations. The newly formed tantalum-based peroxocarbonate ILs displayed a high reactivity and selectivity toward the epoxidation of olefins and allylic alcohols under mild condition. Especially, the conversion between peroxotantalate and Ta-peroxocarbonate species is completely reversible, and CO_2 acts actually as a trigger agent for epoxidation reaction. This unique feature allows this IL catalyst to be recyclable facilely. The DFT calculation indicated further that due to the insertion of CO_2 into the Ta-O bond, the atomic charge of O^{peroxo} becomes more positive, and the covalency of Ta-O^{peroxo} bond is enhanced. These features leads to a higher reactivity of Ta-O^{peroxo} bond in $[Ta(\eta^2\text{-}O_2)_3(CO_4)]^{3-}$ than that in $[Ta(\eta^2\text{-}O_2)_4]^{3-}$ anions. Two possible reaction pathways were investigated and the results indicated that the epoxidation at the η^2-peroxo site was observed to be more competitive than at the peroxocarbonate site. Mononuclear tantalum complexes have received significantly much less attention in the literature as epoxidation catalysts, especially than that of these reported tungsten peroxo complex catalysts.[30] This work is the first example of CO_2-induced metal-based peroxocarbonate ILs. We consider that this catalytically active metal peroxocarbonate ILs remained a huge challenge for mechanic studies and the investigation will inspire the rational design of new ILs for more efficient catalysis from the viewpoint of fundamental science and practical application.

Conflicts of interest

There are no conflicts to declare.

Acknowledgements

The authors are grateful for financial support from the National Natural Science Foundation of China (21373082, 21773061), the Innovation Program of the Shanghai Municipal Education Commission (15ZZ031).

Notes and References

1 (a) H. Furutachi, K. Hashimoto, S. Nagatomo, T. Endo, S. Fujinami, Y. Watanabe, T. Kitagawa and M. Suzuki, J. Am. Chem. Soc., 2005, 127, 4550. (b) K. Hashimoto, S. Nagatomo, S. Fujinami, H. Furutachi, S. Ogo, M. Suzuki, A. Uehara, Y. Maeda, Y. Watanabe and T Kitagawa, Angew. Chem. Int. Ed., 2002, 41, 1202. (c) M. Aresta, I. Tommasi, E. Quaranta, C. Fragale, J. Mascetti, M. Tranquille, F. Galan and M. Fouassier, Inorg. Chem., 1996, 35, 4254. (d) M. Aresta, A. Dibenedetto and I. Tommasi, Eur. J. Inorg. Chem., 2001, 1801. (e) B. S. Lane, M. Vogt, V. J. DeRose and K. Burgess, J. Am. Chem. Soc., 2002, 124, 11946. (f) P. J. Hayward, D. M. Blake, G. Wilkinson and C. J. Nyman, J. Am. Chem. Soc., 1970, 92, 5873. (g) R. E. Dinnebier, S. Vensky and M. Jansen, Chem. Eur. J., 2003, 9, 4391. (h) G. Meier and T. Braun, Angew. Chem. Int. Ed., 2012, 51, 12564. (i) M. Aresta, I. Tommasi, A. Dibenedetto, M. Fouassier and J. Mascetti, Inorg. Chim. Acta., 2002, 330, 63.

2 (a) M. Aresta, E. Quaranta and A. Ciccarese, J. Mol. Catal., 1987, 41, 355. (b) M. Aresta, C. Fragale, E. Quaranta and L. Tommas, J. Chem. Soc., Chem. Commun., 1992, 4, 315. (c) S. Sase, M. Hashimoto and K. Goto, Chem. Lett., 2015, 44, 157.

3 D. Bayot and M. Devillers, Coordin. Chem. Rev., 2006, 250, 2610.

4 (a) R. L. Brutchey, C. G. Lugmair, L. O. Schebaum and T. D. Tilley, J. Catal., 2005, 229, 72. (b) Q. S. Gao, S. N. Wang, Y. C. Ma, Y. Tang, C. Giordano and M. Antonietti, Angew. Chem. Int. Ed., 2012, 51, 961. (c) D. T. Bregante, N. E. Thornburg, J. M. Notestein and D. W. Flaherty, ACS Catal., 2018, 8, 2995. (d) S. S. K. Ma, T. Hisatomi, K. Maeda, Y. Moriya and K. Domen, J. Am. Chem. Soc., 2012, 134, 19993. (e) D. A. Ruddy and T. D Tilley, J. Am. Chem. Soc., 2008, 130, 11088. (f) N. Morlanés and J. M. Notestein, J. Catal., 2010, 275, 191. (g) P. Guillo, M. I. Lipschutz, M. E. Fasulo and T. D. Tilley, ACS Catal., 2017, 7, 2303. (h) J. C. Mohandas, E. A. Hamad, E. Callens, M. K. Samantaray, D. Gajan, A. Gurinov, T. Ma, S. O. Chikh, A. S. Hoffman, B. C. Gates and J. M. Basset, Chem. Sci., 2017, 8, 5650. (i) H. Hamed, Z. Omid, H. Thomas W, Chem. Sci., 2016, 7, 6760.

5 D. R. Mulford, J. R. Clark, S. W. Schweiger, P. E. Fanwick and I. P. Rothwell, Organometallics, 1999, 18, 4448.

6 (a) J. M. Lauzon, P. Eisenberger, S. C. Roşca and L. L. Schafer, ACS Catal., 2017, 7, 5921. (b) J. W. Brandt, E. Chong and L. L. Schafer, ACS Catal., 2017, 7, 6323.

7 (a) E. L. Roux, M. Chabanas, A. Baudouin, A. Mallmann, C. Copéret, E. A. Quadrelli, J. T. Cazat, J. M. Basset, W. Lukens, A. Lesage, L. Emsley and G. J. Sunley, J. Am. Chem. Soc., 2004, 126, 13391. (b) Y. Chen, E. Abou-hamad, A. Hamieh, B. Hamzaoui, L. Emsley and J. M. Basset, J. Am. Chem. Soc., 2015, 137, 588.

8 (a) H. Egami and T. Katsuki, Angew. Chem. Int. Ed., 2008, 47, 5171. (b) H. Egami, T. Oguma and T. Katsuki, J. Am. Chem. Soc., 2010, 132, 5886. (c) S. Q. Shi, Y. G. Chen, J. Gong, Z. M. Dai and L. Y. Qu, Transit. Metal Chem., 2005, 30, 136.

9 (a) Y. Zhu, Q. Wang, R. G. Cornwall and Y. Shi, Chem. Rev., 2014, 114, 8199. (b) L. Graser, R. M. Reich, M. Cokoja, A. Pöthig and F. E. Kühn, Catal. Sci. Technol., 2015, 5, 4772. (c) C. Dai, J. Zhang, C. Huang and Z. Lei, Chem. Rev., 2017, 117, 6929.

10 (a) C. X. Miao, B. Wang, Y. Wang, C. G. Xia, Y. M. Lee, W. Nam and W. Sun, J. Am. Chem. Soc., 2016, 138, 936. (b) M. L. Kuznetsov, B. G. M. Rocha, A. J. L. Pombeiro and G. B. Shul'pin, ACS Catal., 2015, 5, 3823.

11 (a) J. Kim, J. Chun and R. Ryoo, Chem. Commun., 2015, 51, 13102. (b) L. J. Davies, P. McMorn, D. Bethell, P. C. B. Page, F. King, F. E. Hancock and G. J. Hutchings, J. Catal., 2001, 198, 319. (c) M. G. Clerici and M. E. Domine In Liquid Phase Oxidation via Heterogeneous Catalysis: Organic Synthesis and Industrial Applications, M. G. Clerici and O. A. Kholdeeva, Eds.; Wiley: Hoboken, New Jersey, 2013, p. 21.

12 (a) N. E. Thornburg, A. B. Thompson and J. M. Notestein, ACS Catal., 2015, 5, 5077. (b) W. J. Yan, A. Ramanathan, P. D. Patel, S.

K. Maiti, B. B. Laird, W. H. Thompson and B. Subramaniam, J. Catal., 2016, 336, 75. (c) A. J. Bonon, Y. N. Kozlov, J. O. Bahú, R. M. Filho, D. Mandelli and G. B. Shul'pin, J. Catal., 2014, 319, 71.

13 (a) A. S. Novikov, M. L. Kuznetsov, B. G. M. Rocha, A. J. L. Pombeiroa and G. B. Shul'pin, Catal. Sci. Technol., 2016, 6, 1343. (b) B. S. Lane and K. Burgess, Chem. Rev., 2003, 103, 2457. (c) W. F. Wang, Q. S. Sun, D. Q. Xu, C. G. Xia and W. Sun, ChemCatChem., 2017, 9, 420. (d) E. A. Mikhalyova, O. V. Makhlynets, T. D. Palluccio, A. S. Filatov and E. V. R. Akimova, Chem. Commun., 2012, 48, 687. (e) C. X. Miao, B. Wang, Y. Wang, C. G. Xia, Y. M. Lee, W. W. Nam and W. Sun, J. Am. Chem. Soc., 2016, 138, 936. (f) T. Omagari, A. Suzuki, M. Akita and M. Yoshizawa, J. Am. Chem. Soc., 2016, 138, 499. (g) A. M. Zima, O. Y. Lyakin, R. V. Ottenbacher, K. P. Bryliakov and E. P. Talsi, ACS Catal., 2013, 3, 139. (h) R. M. Ballesté and L. Q. Jr, J. Am. Chem. Soc., 2007, 129, 15964. (i) B. Chandra, K. K. Singh and S. S. Gupta, Chem. Sci., 2017, 8, 7545. (g) K. H. Tong, K. Y. Wong and T. H. Chan, Org. Lett., 2003, 5, 3423.

14 (a) R. P. Swatloski, S. K. Spear, J. D. Holbrey and R. D. Rogers, J. Am. Chem. Soc., 2002, 124, 4974. (b) R. D. Rogers and K. R. Seddon, Science, 2003, 302, 792. (c) J. Dupont, Acc. Chem. Res., 2011, 44, 1223. (d) Y. H. Lin, A. D. Zhao, Y. Tao, J. S. Ren and X. G. Qu, J. Am. Chem. Soc., 2013, 135, 4207. (e) Y. X. Qiao, W. B. Ma, N. Theyssen, C. Chen and Z. S. Hou, Chem. Rev., 2017, 117, 6881. (f) W. Mamo, Y. Chebude, C. Márquez-Álvarez, I. Díaz and E. Sastre, Catal. Sci. Technol., 2016, 6, 2766

15 (a) Y. Leng, J. Wang, D. R. Zhu, X. Q. Ren, H. Q. Ge and L. Shen, Angew. Chem., 2009, 121, 174. (b) X. L. Chen, S. B. ouvanhthong, H. Wang and H. W. Zheng, Appl. Catal. B-Environ., 2013, 138, 161. (c) Q. Y. Zeng, A. Mukherjee, P. Müller, R. D. Rogers and A. S. Myerson, Chem. Sci., 2018, 9, 1510. (d) M. Li, M. Zhang, A. Wei, W. S. Zhu, S. H. Xun, Y. N. Li, H. P. Li and H. M. Li, J. Mol. Catal. A: Chem., 2015, 406, 23.

16 W. B. Ma, C. Chen, K. Kong, Q. F. Dong, K. Li, M. M. Yuan, D. F. Li and Z. S. Hou, Chem. Eur. J., 2017, 23, 7287.

17 G. Adamová, R. L. Gardas, M. Nieuwenhuyzen, A. V. Puga, L. P. N. Rebelo, A. J. Robertsond and K. R. Seddon, Dalton Trans., 2012, 41, 8316.

18 (a) R. Zhang, L. Guo, J. Z. Chen, H. M. Gan, B. N. Song, W. W. Zhu, L. Hua and Z. S. Hou, ACS Sustainable Chem. Eng., 2014, 2, 1147. (b) Y. Xiang and J. Shen, NMR Biomed., 2011, 24, 1054. (c) F. Mani, M. Peruzzinib and P. Stoppioni, Green Chem., 2006, 8, 995.

19 (a) D. E. Richardson, H. Yao, K. M. Frank and D. A. Bennett, J. Am. Chem. Soc., 2000, 122, 1729. (b) S. Zhao, H. Xi, Y. Zuo, Q. Wang, Z. Wang and Z. Yan, J. Hazard. Mater., 2018, 344, 136.

20 M. A. Moreno, B. Maté, Y. Rodríguez-Lazcano, O. Gálvez, P. C. Gómez, V. J. Herrero and R. Escribano, J. Phys. Chem. A., 2013, 117, 9564.

21 A. Pulido, M. R. Delgado, O. Bludský, M. Rubeš, P. Nachtigall and C. O. Areán, Energy Environ. Sci., 2009, 2, 1187.

22 B. C. Dunn, J. Marda and E. M. Eyring, Appl. Spectrosc., 2002, 56, 751.

23 T. Cao, L. Sun, Y. Shi, L. Hua, R. Zhang, L. Guo, W. Zhu and Z. S. Hou, Chin. J. Catal., 2012, 33, 416.

24 (a) B. R. Goldsmith, T. Hwang, S. Seritan, B. Peters and S. L. Scott, J. Am. Chem. Soc., 2015, 137, 9604. (b) W. B. Ma, H. Y. Yuan, H. F. Wang, Q. Q. Zhou, K. Kong, D. F. Li, Y. F. Yao and Z. S. Hou, ACS Catal., 2018, 8, 4645.

25 N. V. Maksimchuk, G. M. Maksimov, V. Y. Evtushok, I. D. Ivanchikova, Y. A. Chesalov, R. I. Maksimovskaya, O. A. Kholdeeva, A. S. Daura, J. M. Poblet and J. J. Carbó, ACS Catal., 2018, 8, 9722.

26 (a) C. Chen, H. Y. Yuan, H. F. Wang, Y. F. Yao, W. B. Ma, J. Z. Chen and Z. S. Hou, ACS Catal., 2016, 6, 3354. (b) K. Kamata, K. Yamaguchi and N. Mizuno, Chem. Eur. J., 2004, 10, 4728.

27 (a) M. Papastergiou, P. Stathi, E. R. Milaeva, Y. Deligiannakis and M. Louloudi, J. Catal., 2016, 341, 104. (b) W. W. Cheng, G. Q. Liu, X. D. Wang, X. Q. Liu and L. Jing, Eur. J. Lipid Sci. Technol., 2015, 117, 1185. (c) G. G. Allan and A. N. Neogi, J. Catal., 1970, 16, 197.

28 (a) K. Morokuma, J. Chem. Phys., 1971, 55, 1236. (b) K. Kitaura and K. Morokuma, Int. J. Quantum Chem., 1976, 10, 325.

29 T. Ziegler and A. Rauk, Theor. Chim. Acta., 1977, 46, 1.

30 (a) Z. P. Pai, D. Y. Yushchenko, T. B. Khlebnikova and V. N. Parmon, Catal. Commun., 2015, 71, 102. (b) K. Kamata, K. Sugahara, K. Yonehara, R. Ishimoto and N. Mizuno, Chem. Eur. J., 2011, 17, 7549. (c) K. Kamata, T. Hirano, S. Kuzuya and N. Mizuno, J. Am. Chem. Soc., 2009, 131, 6997.

View Article Online
DOI: 10.1039/C9CY00056A

Table of Contents

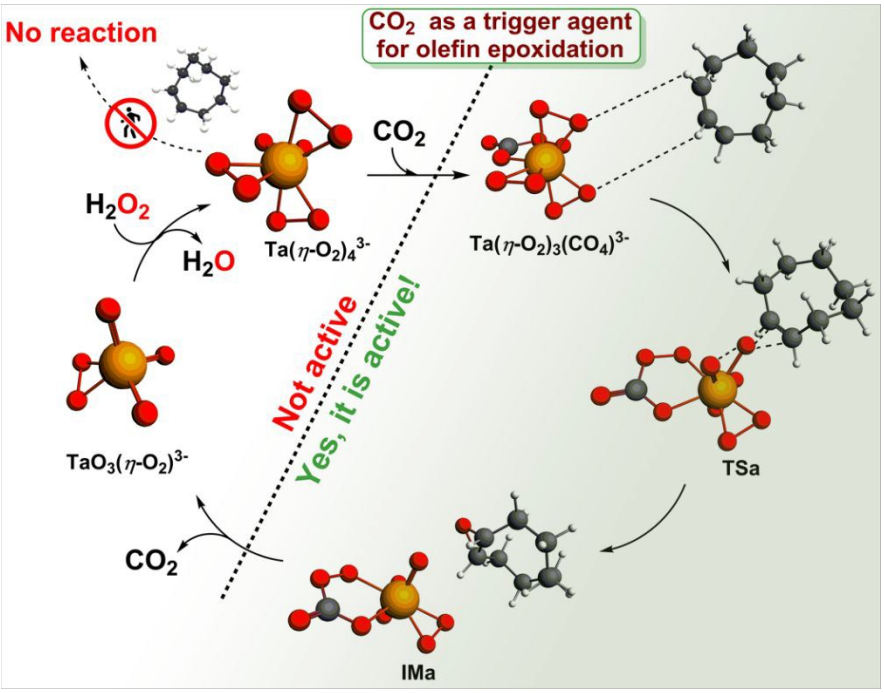

Mononuclear tantalum complex tethering a peroxocarbonate ligand has been proved to be particularly important in the epoxidation reactions.